

Spectroscopic evidence for preformed Cooper pairs in the pseudogap phase of cuprates

M. Shi,¹ A. Bendounan,² E. Razzoli,¹ S. Rosenkranz,³ M. R. Norman,³ J. C. Campuzano,^{4,3} J. Chang,² M. Månsson,^{5,6} Y. Sassa,² T. Claesson,⁶ O. Tjernberg,⁶ L. Patthey,¹ N. Momono,⁷ M. Oda,⁷ M. Ido,⁷ S. Guerrero,⁸ C. Mudry,⁸ and J. Mesot²

¹Swiss Light Source, Paul Scherrer Institute, CH-5232 Villigen PSI, Switzerland

²Paul Scherrer Institute, ETH Zurich and EPF Lausanne, 5232 Villigen PSI, Switzerland

³Materials Science Division, Argonne National Laboratory, Argonne, IL 60439 USA

⁴Department of Physics, University of Illinois at Chicago, Chicago, IL 60607 USA

⁵Laboratory for Neutron Scattering, ETH Zurich and Paul Scherrer Institute, CH-5232 Villigen PSI, Switzerland

⁶Materials Physics, Royal Institute of Technology KTH, S-164 40 Kista, Sweden

⁷Department of Physics, Hokkaido University Sapporo 060-0810, Japan

⁸Condensed Matter Theory Group, Paul Scherrer Institute, CH-5232 Villigen PSI, Switzerland

(Dated: November 8, 2018)

Angle-resolved photoemission on underdoped $\text{La}_{1.895}\text{Sr}_{0.105}\text{CuO}_4$ reveals that in the pseudogap phase, the dispersion has two branches located above and below the Fermi level with a minimum at the Fermi momentum. This is characteristic of the Bogoliubov dispersion in the superconducting state. We also observe that the superconducting and pseudogaps have the same d -wave form with the same amplitude. Our observations provide direct evidence for preformed Cooper pairs, implying that the pseudogap phase is a precursor to superconductivity.

PACS numbers: 74.72.Dn, 74.25.Jb, 79.60.Bm

In conventional superconductors, the energy gap decreases with increasing temperature and vanishes at T_c . For the high temperature cuprates, the situation is more complicated. In the underdoped region, an energy gap, known as the pseudogap, persists above T_c , its maximum amplitude remaining unchanged before the gap fills in at a temperature, T^* [1, 2]. Both T^* and the pseudogap increase with reduced doping, whereas T_c decreases. In spite of much effort, there is no consensus on the origin of the pseudogap [3]. One idea is that the energy gap above T_c is indicative of preformed Cooper pairs [4, 5] that only become phase coherent below T_c . A competing view is that the pseudogap results from some other order which competes with superconductivity. In this picture, the superconducting gap only exists along gapless Fermi arcs [6, 7, 8, 9], and as in conventional superconductors, it closes at T_c . Using angle-resolved photoemission spectroscopy (ARPES), we show the existence of a Bogoliubov-like dispersion in the pseudogap phase of the underdoped cuprate $\text{La}_{1.895}\text{Sr}_{0.105}\text{CuO}_4$. This provides direct evidence that the pseudogap is a signature of preformed Cooper pairs above T_c .

ARPES experiments were carried out at the Surface and Interface Spectroscopy beamline at the Swiss Light Source on single crystals of underdoped $\text{La}_{1.895}\text{Sr}_{0.105}\text{CuO}_4$ (LSCO) with $T_c = 30\text{K}$ and overdoped $\text{Bi}_2\text{Sr}_2\text{CaCu}_2\text{O}_{8+\delta}$ (Bi2212) with $T_c = 65\text{K}$, grown using the travel solvent floating method. Circularly polarized light with $h\nu = 55\text{eV}$ and linearly polarized light with $h\nu = 21.2\text{eV}$ were used for LSCO and Bi2212, respectively. The energy and angle resolutions were 17 meV and 0.1 - 0.15°. The Fermi level was determined by recording the photoemission spectra from

polycrystalline copper on the sample holder. For LSCO, the samples were cleaved in situ by using a specially designed cleaver [10].

In Fig. 1 we show spectra obtained below and above T_c from angle resolved photoemission spectroscopy (ARPES) for underdoped $\text{La}_{1.895}\text{Sr}_{0.105}\text{CuO}_4$ ($T_c=30\text{K}$) near the node (Fig. 1(a), (d)), near the anti-node (Fig. 1(c), (f)), and in between (Fig. 1(b), (e)). Here, the node refers to where the d -wave superconducting gap vanishes, with the anti-node where it is maximal. To determine the Fermi momentum k_F and the energy gap, we symmetrize the spectra along each cut [11], $A(\omega) = I(\omega) + I(-\omega)$, where $I(\omega)$ is the measured intensity at the energy ω . k_F was identified by searching for the minimum gap location of the symmetrized spectra along a given cut in momentum space. The same underlying Fermi surface was obtained by analyzing the spectra in the superconducting state and in the pseudogap phase. The energy gap at a given k_F was determined by fitting the symmetrized spectrum (Fig. 1(g)), with the spectral function calculated from a model self-energy [12] of the form $\Sigma = -i\Gamma_1 + \Delta^2/(\omega + i0^+)$, and then convolved with the instrumental resolution. Like for lightly underdoped $\text{La}_{1.855}\text{Sr}_{0.145}\text{CuO}_4$ [13], the superconducting gap at $T = 12\text{K}$ traces out a simple d -wave form with a maximum amplitude of 25 meV at the anti-node (Fig. 1(i)). Above T_c at $T = 49\text{K}$, there is a small gapless Fermi arc near the node (Fig. 1(h), (i)). Beyond the Fermi arc, a pseudogap is present that follows the same simple d -wave form as the superconducting gap. It is interesting to note that in our spectral fits, the inverse lifetime, Γ_1 , has the same angular anisotropy as the energy gap (Fig. 1(i), (k)). Similar results have been inferred from fits to scanning tunneling

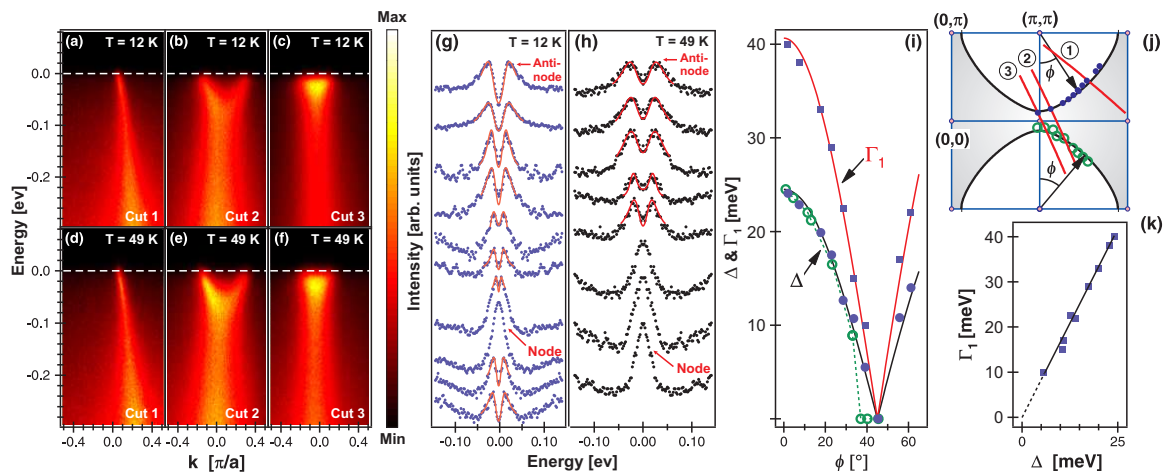


FIG. 1: (Color online) ARPES spectra for underdoped $\text{La}_{1.895}\text{Sr}_{0.105}\text{CuO}_4$ ($T_c = 30\text{K}$). (a)-(c): ARPES intensities at $T = 12\text{K}$ along momentum cuts that cross the Fermi surface at the node, between the node and the anti-node, and at the anti-node. The corresponding cuts are indicated in (j). (d)-(f): the same as (a)-(c), but the spectra are acquired at 49K. (g)-(h): the symmetrized spectra for various k_F from the anti-node (top) to the node (bottom) at 12K and 49K, respectively. The solid curves are fits. In (g), the node is the third spectrum from the bottom, with the bottom two on the other side of the node. (i) The superconducting gap (filled circles) at 12K and the pseudogap (open circles) at 49K, as a function of the Fermi surface angle (ϕ), with the solid curve the simple d -wave form $\Delta_{max} \cos(2\phi)$ with $\Delta_{max} = 25\text{meV}$. The squares are the values of the inverse lifetime, Γ_1 , at 12K, which also follows a simple d -wave form (solid curve). (j) The Fermi surface at 12K (filled circles) and at 49K (open circles). The solid line is a tight-binding fit. (k) Scaling of Γ_1 with Δ at 12K with an extrapolation to the node by the dashed line.

microscopy data below T_c [14], and photoemission data, both below T_c [15] and also above T_c in the pseudogap phase [16].

Fig. 2 demonstrates the different dispersions in the pseudogap phase along two momentum cuts, one where the spectrum is gapped (cut 1 in Fig. 2(e)) and the other which intersects the gapless Fermi arc (cut 2 in Fig. 2(e)). As the spectra were acquired at $T = 49\text{K}$, there is appreciable thermal population above the Fermi energy (E_F), which allows us to follow the dispersions through E_F . To trace the dispersion in the vicinity of E_F (Fig. 2(j)), we divide the raw ARPES spectra by the instrumental resolution broadened Fermi function, and then follow the peak positions of the divided spectra. When the spectral peak is weak and sits on a sloped background (for the lowest two curves in Fig. 2(d)), we first fit the spectrum with polynomials to high precision and then use the second derivative of the fitted curve to determine the peak position. Along cut 2, the spectral peak of the Fermi function divided data continuously moves to higher energies and crosses E_F at the underlying k_F (Fig. 2(i)). The dispersion resembles that of a normal metal. On the other hand, the dispersion along cut 1 shows a remarkable difference to that along cut 2. As shown in Fig. 2(c), from top to bottom curves, the spectral peak approaches E_F before k reaches the underlying k_F and then it recedes to higher binding energies and loses spectral weight. Fig. 2(d) shows the Fermi function divided data along cut 1. The dispersion along this cut has two

branches, separated by an energy gap, moving in opposite directions: one is above E_F and the other is below. As k approaches the underlying k_F from the occupied side, the spectral weight of the upper branch increases. The spectral peaks of the two branches have approximately the same weight at k_F , and at the same location, the energy gap between the two branches is minimal, giving rise to a flat topped spectrum. All of this is characteristic of the Bogoliubov-like dispersion seen previously below T_c [17, 18]. But, away from k_F , the peaks in the lower and upper branches are slightly asymmetric in energy relative to E_F (Fig. 2(j)). This may result from an asymmetry of the self-energy in the pseudogap phase, which would act to broaden the spectral peaks and shift them to slightly higher binding energy on the occupied side. To illustrate this, in Fig. 2(d), we overlay the spectra obtained in the superconducting state (the thin lines) on those in the pseudogap phase. It can be seen that the peak positions of the Fermi function divided spectra in the superconducting state are at a lower binding energy, and the dispersion is now symmetric relative to E_F to that of the upper branch determined in the pseudogap phase. It should be mentioned that in the gapped region of the zone in the pseudogap phase, all dispersions obtained from the Fermi function divided spectra show a back bending at k_F (Fig. 2(j)), one of the characteristics of the Bogoliubov-like dispersion. However, when the energy gap amplitude becomes too large near the anti-node, only the lower branch of the dispersion can

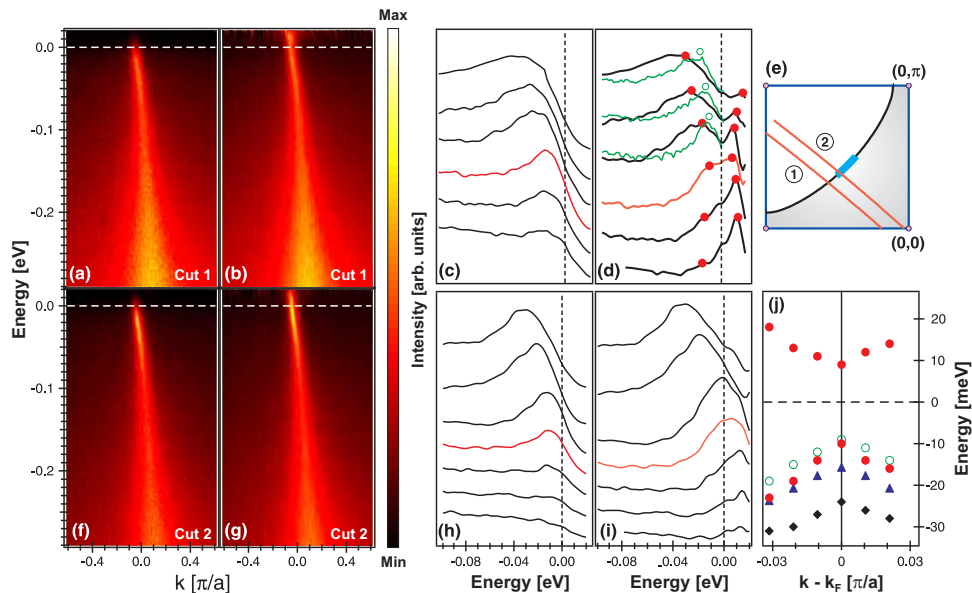


FIG. 2: (Color online) ARPES spectra for underdoped $\text{La}_{1.895}\text{Sr}_{0.105}\text{CuO}_4$ at 49K. (a)-(d): the spectra along cut 1 in (e). (a) the ARPES intensity, (b) the intensity divided by the resolution broadened Fermi function, (c) the spectra in the vicinity of k_F , and (d) the Fermi function divided spectra. The thick and thin lines in (d) are the spectra at 49K and 12K, respectively. The closed and open circles indicate the spectral peak positions. (e) Fermi surface and locations of cuts 1 and 2. The thick line centered at the node indicates the gapless Fermi arc. (f)-(i): the same as (a)-(d), but the spectra are along cut 2 in (e). (j) The dispersions in the gapped region of the zone obtained from the Fermi function divided spectra. The pair of closed circles are the two branches of the dispersion derived from (d) at 49K, the dispersion indicated with open circles is along the same cut (cut 1 in (e)) but at 12K. The curves indicated by triangles and diamonds are the dispersions at 49K in the vicinity of the lower underlying Fermi surface along cut 2 and 3 in Fig. 1(j), respectively.

be measured. Similar back bent dispersions have been reported for underdoped Bi2212 above T_c [19]. We note that the spectral peaks above E_F are narrower than those below - this may be due to the asymmetry effect we noted above, or could be an artifact of the Fermi function division process, which is not an exact procedure because the observed spectra result from a convolution with the instrumental resolution function.

The spectral change from cut 1 to cut 2 in Fig. 2(e) is similar to the spectral change from the superconducting state to the normal state of overdoped cuprates which do not have a pseudogap above T_c . To demonstrate this, we present in Fig. 3 ARPES spectra (also divided by the resolution broadened Fermi function) along the momentum cut shown in Fig. 3(e) on a heavily overdoped $\text{Bi}_2\text{Sr}_2\text{CaCu}_2\text{O}_{8+\delta}$ (Bi2212) sample with $T_c = 65\text{K}$ and a maximum superconducting gap, $\Delta_{max} = 24\text{meV}$, similar to that of underdoped $\text{La}_{1.895}\text{Sr}_{0.105}\text{CuO}_4$. Above T_c , the spectral peak of the Fermi function divided spectra shows a linear dispersion going through k_F (Fig. 3(g), (i)). Below T_c (Fig. 3(b), (d)), the superconducting gap opens up and the linear dispersion of the normal state transforms into the Bogoliubov dispersion of the superconducting state: $E_k = \pm\sqrt{\epsilon_k^2 + \Delta_k^2}$, where ϵ_k is the energy band dispersion in the normal state and Δ_k is the gap function. The double branches in the electronic excitation spectra involve mixtures of electron and hole states, the spectral

weight in the lower (upper) branch is proportional to v^2 (u^2) through the relation $u^2 = 1 - v^2 = \frac{1}{2}(1 + \epsilon_k/E_k)$, where u and v are the coherence factors [17, 18]. At the normal state k_F , the lower (upper) branch of the Bogoliubov dispersion reaches its maximum (minimum), and the two branches have equal spectral weight. Remarkably, like in overdoped Bi2212, the two branches of the dispersion along cut 1 in the pseudogap phase of underdoped $\text{La}_{1.895}\text{Sr}_{0.105}\text{CuO}_4$ possess all of these properties.

To summarize, our main experimental findings are: 1) beyond the gapless Fermi arc, the pseudogap above T_c has the same simple d -wave form as the superconducting gap below T_c , 2) above T_c there exists a Bogoliubov-like dispersion near the underlying k_F where the spectra are gapped, and 3) the same underlying Fermi surface was obtained both in the superconducting state and in the pseudogap phase. In the pseudogap phase, the low energy electronic excitations along this cut are well defined both in energy and in momentum (Fig. 2(a)-(d)). Thus our experimental results can readily rule out the possibility that the pseudogap in underdoped cuprates only exists in the anti-nodal region, which has been attributed to a competing order such as charge ordering [20]. Our experimental findings are also inconsistent with a wide range of scenarios where the pseudogap originates from some ordering phenomenon associated with a non-zero Q vector [21]. In our ARPES spectra, we do not find any

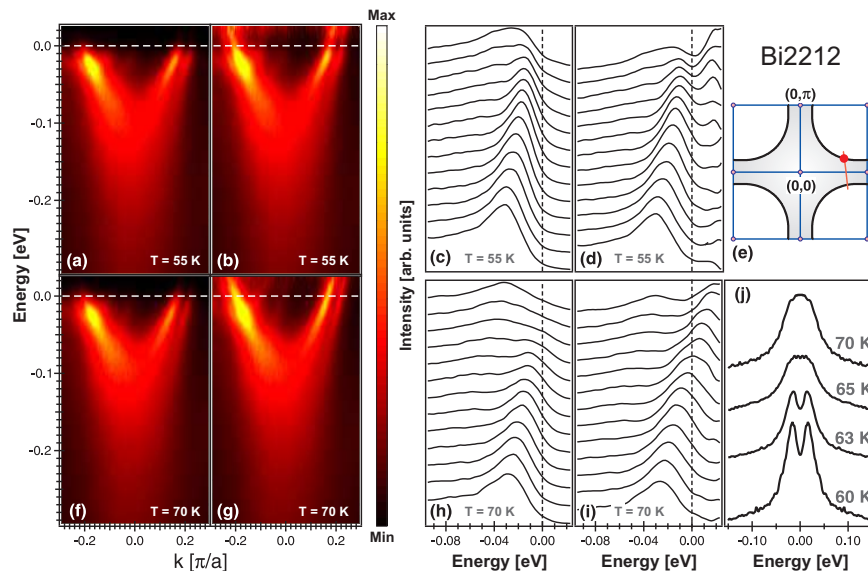


FIG. 3: (Color online) ARPES spectra for overdoped $\text{Bi}_2\text{Sr}_2\text{CaCu}_2\text{O}_{8+\delta}$ ($T_c = 65\text{K}$). (a)-(d): the spectra taken at 55K along the cut in (e). (a) the ARPES intensity, (b) the intensity divided by the resolution broadened Fermi function, (c) the spectra in the vicinity of k_F (solid dot in (e)), and (d) the Fermi function divided spectra. (e) The Fermi surface and the location of the cut. (f)-(i): the same as (a)-(d), but the spectra are taken at 70K. (j) the symmetrized spectra at the anti-node at various temperatures. The superconducting gap closes at T_c .

signature of additional (shadow) states that are displaced by a non-zero Q , neither in the pseudogap phase nor in the superconducting state. It should be mentioned that in the pseudogap phase, the dispersion in the anti-nodal region also bends back at the underlying k_F (Fig. 2(j)). However, due to the large amplitude of the pseudogap near the anti-node, the upper branch of the Bogoliubov-like dispersion is not thermally populated at 49K, and thus cannot be identified by Fermi function division.

Our experimental results support the idea that the pseudogap originates from preformed Cooper pairs for $T > T_c$. However, because the energy gap is larger than the phase stiffness in the pseudogap phase, the preformed pairs have a finite lifetime and can not travel in the crystal coherently. The similarity between the Bogoliubov-like dispersion in the pseudogap phase of underdoped $\text{La}_{1.895}\text{Sr}_{0.105}\text{CuO}_4$ and the dispersion of Bogoliubov quasiparticles in the superconducting state of heavily overdoped Bi2212 provides direct evidence that the pseudogap in underdoped cuprates arises from pairing of electrons, and thus the pseudogap phase is a state precursor to superconductivity. Because the superconducting and pseudogaps have the same simple d -wave form along the underlying Fermi surface beyond the Fermi arc (Fig. 1(i)), it is difficult to image that there is some k_F located between the anti-node and the end of the Fermi arc at which the pseudogap changes its nature from preformed Cooper pairs near the arc to competing order near the anti-node. It is more reasonable to infer that there is a single pseudogap above T_c which transforms into the superconducting gap below T_c .

This work was supported by the Swiss National Sci-

ence Foundation (through NCCR, MaNEP, and grant Nr 200020-105151), the Ministry of Education and Science of Japan, the Swedish Research Council, the U.S. DOE, Office of Science, under Contract No. DE-AC02-06CH11357, and by NSF DMR-0606255. We thank the beamline staff of X09LA at the SLS for their excellent support.

-
- [1] A. G. Loeser *et al.*, Science **273**, 325 (1996).
 - [2] H. Ding *et al.*, Nature **382**, 51 (1996).
 - [3] M. R. Norman, D. Pines and C. Kallin, Adv. Phys. **54**, 715 (2005).
 - [4] M. Randeria *et al.*, Phys. Rev. Lett. **69**, 2001 (1992).
 - [5] V. J. Emery and S. A. Kivelson, Nature **374**, 434 (1995).
 - [6] K. Tanaka *et al.*, Science **314**, 1910 (2006).
 - [7] T. Kondo *et al.*, Phys. Rev. Lett. **98**, 267004 (2007).
 - [8] K. Terashima *et al.*, Phys. Rev. Lett. **99**, 017003 (2007).
 - [9] W. S. Lee *et al.*, Nature **450**, 81 (2007).
 - [10] M. Månsson *et al.*, Rev. Sci. Instr. **78**, 076103 (2007).
 - [11] M. R. Norman *et al.*, Nature **392**, 157 (1998).
 - [12] M. R. Norman *et al.*, Phys. Rev. B **57**, 11093 (1998).
 - [13] M. Shi *et al.*, Phys. Rev. Lett. **101**, 047002 (2008).
 - [14] J. W. Alldredge *et al.*, Nat. Phys. **4**, 319 (2008).
 - [15] J. Chang *et al.*, arXiv:0708.2782.
 - [16] A. Kaminski *et al.*, Phys. Rev. B **71**, 014517 (2005).
 - [17] J. C. Campuzano *et al.*, Phys. Rev. B **53**, 14737 (1996).
 - [18] H. Matsui *et al.*, Phys. Rev. Lett. **90**, 217002 (2003).
 - [19] A. Kanigel *et al.*, Phys. Rev. Lett. **101**, 137002 (2008).
 - [20] K. M. Shen *et al.*, Science **307**, 901 (2005).
 - [21] M. R. Norman *et al.*, Phys. Rev. B **76**, 174501 (2007).